# Ship Detection Using SAR and AIS Raw Data for Maritime Surveillance

Fábio Manzoni Vieira[(1),(2)], François Vincent[(1),(2)], Jean-Yves Tourneret[(1),(3)], David Bonacci[(1)],
Marc Spigai[(4)], Marie Ansart[(4)] and Jacques Richard[(4)]

[(1)]TéSA Laboratory, 7 boulevard de la Gare, 31500 Toulouse, France, {fabio.manzoni; firstname.surname}@tesa.prd.fr
[(2)]ISAE, Dep. of Electronics, Optronics and Signal, Univ. of Toulouse, France, {firstname.surname}@isae.fr
[(3)]INP-ENSEEIHT/IRIT, University of Toulouse, France, jean-yves.tourneret@enseeiht.fr
[(4)]Thales Alenia Space, 26 Av. J.F. Champollion, 31100 Toulouse, France, {firstname.surname}@thalesaleniaspace.com

*Abstract*—**This paper studies a maritime vessel detection method based on the fusion of data obtained from two different sensors, namely a synthetic aperture radar (SAR) and an automatic identification system (AIS) embedded in a satellite. Contrary to most methods widely used in the literature, the present work proposes to jointly exploit information from SAR and AIS raw data in order to detect the absence or presence of a ship using a binary hypothesis testing problem. This detection problem is handled by a generalized likelihood ratio detector whose test statistics has a simple closed form expression. The distribution of the test statistics is derived under both hypotheses, allowing the corresponding receiver operational characteristics (ROCs) to be computed. The ROCs are then used to compare the detection performance obtained with different sensors showing the interest of combining information from AIS and radar.**

*Index Terms*—**multi-sensor fusion, detection, automatic identification system (AIS), synthetic aperture radar (SAR), maritime surveillance**

## I. Introduction

Maritime surveillance has been receiving a growing interest during the recent years [1], [2]. It can be performed with information from vessel monitoring systems based on cooperative transmitting technologies or from detection sensors. Cooperative sources are equipped with electronic navigation sensors in order to estimate the position of a ship (usually a global navigation satellite system (GNSS) or an inertial sensor), and with radio equipment for communication purposes. Conversely, one usually relies on remote sensing equipments such as radars or image sensors for non-cooperative scenarios. These equipments can be deployed in coastal stations, surveillance ships, aircraft and satellites.

The automatic identification system (AIS) is a mandatory communication system required for some cargo ships and for all passenger ships regardless of their size [3]. The AIS is used to broadcast ship information to nearby vessels. This information is related to the ship itself (including its identity, position, size, direction, speed, timestamp) but also includes other features such as the sea state. The nominal reporting interval depends on the ship dynamic conditions, which can vary from 3 minutes (for anchored ships not moving faster than 3 knots) to 2 seconds (e.g., for ships whose speed is greater than 23 knots). Originally designed as an anti-collision system for large vessels, the AIS by satellite has been proved

to be viable [4], [5]. As a consequence, AIS transponders have been included in many satellites [6], [7]. The AIS broadcasts are continuously harvested by sea ports, surveillance ships and satellites, and the information is used for registering, traffic monitoring, safety and surveillance. The satellite AIS coverage is close to the size of the satellite footprint because AIS satellite reception is possible at low elevation angles. For reference, a low orbit satellite (whose altitude goes from 200 km to 2.000 km) has a footprint between 1.5% and 12% of the Earth's surface area [8].

On the other hand, synthetic aperture radar (SAR) sensors embedded in satellites are a common choice for ship detection and imaging. They are recognized for their high resolution properties, independence from sunlight, resistance to adverse atmospheric conditions and coverage from tens to few hundreds of kilometers of swath width [2].

Despite providing useful information, cooperative systems alone are not fully appropriate for maritime surveillance because of the diversity of surveillance scenarios and the presence of non-cooperative targets. Just as an example, in scenarios with illicit activities such as piracy, illegal fishing, smuggling, cooperative data can be counterfeit, masked or even not transmitted at all (small boats). On the other hand, non-cooperative systems are less sensitive to deception in non-military situations (without radar furtiveness or countermeasures) and thus have proved to be useful for some specific maritime surveillance scenarios [9], [10]. However, there are still lots of remaining challenges related to maritime surveillance using only non-cooperative systems since information recovery is limited and the detections need to be interpreted somehow. These challenges include ship detection, identification and tracking, or speed and heading estimation. Furthermore, some non-cooperative systems have limited coverage and their reliability can vary with environmental conditions, e.g., related to sea clutter.

For all reasons mentioned above, the use of different sources of information is a natural choice to overcome the individual sensor limitations and manage both cooperative and non-cooperative targets. However, processing data acquired by different sensors requires an appropriate data fusion strategy in order to obtain high performance maritime surveillance. Data fusion systems can exploit the complementary informa-

tion associated with different sensors in several ways. The conventional approach considers data fusion after detection, where the detectors provide lists of detections that need to be merged together. Some features that can be used for data fusion include ship position, heading and speed among others (see [2], [10]–[12] for more details). In this paper we propose to fuse the data at an upstream step of the processing. Indeed, the closer to the raw data, the less loss of information due to processing. This way, one can expect better performance and possibly detect smaller targets that would have been discarded by the conventional detector. In a fusion-before-detect scheme, we study a new detector adapted to raw data acquired by both AIS and SAR sensors.

The paper is organized as follows. Section II introduces statistical models associated with the signals acquired by the AIS and SAR sensors. Section III investigates a generalized likelihood ratio test (GLRT) for the detection of a ship by using signals acquired by AIS and SAR sensors. Section IV studies the distribution of the GLRT detector under two hypotheses associated with the absence or presence of a ship. Section V evaluates the theoretical performance of the proposed detector in different scenarios corresponding to ships of different sizes. Conclusions and future work are finally reported in Section VI.

## II. DATA MODEL

### A. AIS signal

The AIS default packet length is 256 bits of data and signaling bits. However, the bit-stuffing operation used in the AIS protocol [13] possibly increases the packet length by adding extra bits to the data stream in order to preserve signal transitions (necessary to synchronize the receiver clock) and also to avoid the appearance of signaling pattern inside the data bit stream [14]. The bits are then NRZI encoded and modulated using a Gaussian minimum shift keying (GMSK) modulation before message transmission. An attenuated, delayed and Doppler shifted version of the transmitted AIS signal is then received by the AIS satellite. Note that a possible overlap of AIS transmissions may occur due to the high number of ships seen by a satellite (AIS message collisions).

This paper directly considers the raw AIS signal acquired by the receiver. This signal is a vector of complex time samples obtained after in-phase and quadrature (I/Q) demodulation before any signal processing step. For a single vessel at a position $\boldsymbol{\theta} = (x, y)^T \in \mathbb{R}^2$, the received sampled AIS signal $\boldsymbol{y}_{\mathrm{AIS}} = (\boldsymbol{y}_{\mathrm{AIS}}(1), ..., \boldsymbol{y}_{\mathrm{AIS}}(N_{\mathrm{AIS}}))^T \in \mathbb{C}^{N_{\mathrm{AIS}}}$ (where $N_{\mathrm{AIS}}$ is the sample size) is defined as

$$\boldsymbol{y}_{\mathrm{AIS}} = \beta \boldsymbol{b}(\boldsymbol{\theta}) + \boldsymbol{n}_{\mathrm{AIS}} \tag{1}$$

where $\boldsymbol{b}(\boldsymbol{\theta}) \in \mathbb{C}^{N_{\mathrm{AIS}}}$ represents the AIS signal vector for a ship located at position $\boldsymbol{\theta}$, $\beta \in \mathbb{C}$ is the unknown complex signal amplitude and $\boldsymbol{n}_{\mathrm{AIS}} \in \mathbb{C}^{N_{\mathrm{AIS}}}$ is the additive measurement noise. We assume here that the noise sequence contains uncorrelated complex white Gaussian samples, i.e., $\boldsymbol{n}_{\mathrm{AIS}} \sim \mathcal{CN}\left(0, \sigma_{\mathrm{AIS}}^2 \boldsymbol{I}_{N_{\mathrm{AIS}}}\right)$, where $\boldsymbol{I}_{N_{\mathrm{AIS}}}$ is the $N_{\mathrm{AIS}} \times N_{\mathrm{AIS}}$ identity matrix.

The AIS message is unknown but contains some bits that can be predicted [1]. As a consequence, the AIS signal model $\boldsymbol{b}(\boldsymbol{\theta})$ can be constructed using the known signaling bits (here the "training sequence", "start flag" and the "end flag") and the predicted message bits (here "latitude" and "longitude" bits in the AIS message). The remaining bits are blanked (replaced by zeros) and thus do not impact the detection performance.

### B. SAR signal

A SAR system typically uses linear frequency modulated pulses $\psi(t) = 1_T(t)e^{j\gamma t^2}$ (where $1_T(t)$ is the indicator function on the interval $]-T/2, +T/2[$ and $\gamma$ is the chirp rate parameter). During the azimuth displacement of the satellite, the SAR illuminates a side-looking target area on the Earth surface with a burst of $N_P$ pulses modulated by a carrier frequency $f_0$ (see Fig. 1). The transmitted SAR signal can be written

$$s(t) = \sum_{h=1}^{N_P} \psi(t - hT_i)e^{j2\pi f_0 t}$$

where $T_i$ is the pulse repetition interval. The signal acquired by the receiver is the sum of all scattered echoes from the illuminated targets. For a single target at some position $\boldsymbol{\theta}$, the received signal is $Ar(t) = As(t - \tau_{\boldsymbol{\theta}}(t))$, where the scalar $A$ is an attenuation factor due to the propagation losses, $\tau_{\boldsymbol{\theta}}(t)$ is the time delay expressed as function of the distance to the target $\tau_{\boldsymbol{\theta}}(t) = 2R_{\boldsymbol{\theta}}(t)/c$ with $R_{\boldsymbol{\theta}}(t) = \|\vec{P}(t) - \vec{Q}(t)\|$ and $c$ is the speed of light. The term $\tau_{\boldsymbol{\theta}}(t)$ induces a Doppler associated with the received signal $r(t)$ due to the satellite radial speed relative to the ship $\dot{R}_{\boldsymbol{\theta}}(t)/c$.

In this paper, we directly consider the raw radar signal which is a vector of complex time samples obtained after I/Q demodulation and before any signal processing. For a single vessel at position $\boldsymbol{\theta} = (x, y)^T \in \mathbb{R}^2$, the received sampled radar signal $\boldsymbol{y}_{\mathrm{rad}} = (\boldsymbol{y}_{\mathrm{rad}}(1), ..., \boldsymbol{y}_{\mathrm{rad}}(N_{\mathrm{rad}}))^T \in \mathbb{C}^{N_{\mathrm{rad}}}$ is defined as

$$\boldsymbol{y}_{\mathrm{rad}} = \alpha \boldsymbol{a}(\boldsymbol{\theta}) + \boldsymbol{n}_{\mathrm{rad}} \tag{2}$$

where $\boldsymbol{a}(\boldsymbol{\theta}) = (r(t_1), ..., r(t_{N_{\mathrm{rad}}}))^T$ (with $t_1, ..., t_{N_{\mathrm{rad}}}$ the sampling times), the scalar $\alpha$ is the unknown complex signal amplitude and $\boldsymbol{n}_{\mathrm{rad}}$ is the additive measurement noise whose components are uncorrelated complex white Gaussian samples, i.e., $\boldsymbol{n}_{\mathrm{rad}} \sim \mathcal{CN}\left(0, \sigma_{\mathrm{rad}}^2 \boldsymbol{I}_{N_{\mathrm{rad}}}\right)$.

### C. Modeling assumptions

In order to simplify the detection scenario, we consider the following assumptions

**Assumption 1**: At a given time instant $t$, the AIS and radar signals are synchronous with respect to the ship position $\boldsymbol{\theta}(t) = [x(t), y(t)]^T$, where the time dependence of $\theta, x$ and $y$ has been outlined here for clarity. As the signals coming from the same ship are usually acquired by the SAR and AIS sensors at distinct time instants $t_{\mathrm{rad}} \neq t_{\mathrm{AIS}}$, they do not generally correspond to the same coordinates. However, we assume here that these coordinates have been corrected in order to obtain $\boldsymbol{\theta}(t_{\mathrm{AIS}}) = \boldsymbol{\theta}(t_{\mathrm{rad}})$. It is worth noting that the equality
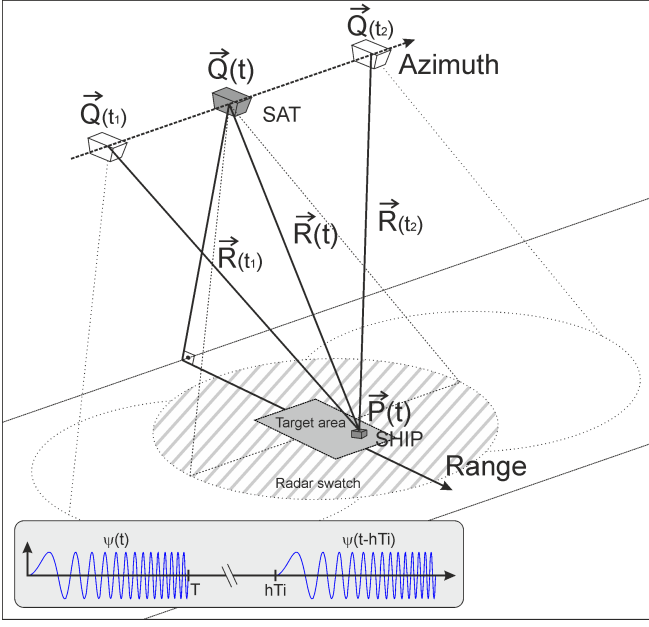
Fig. 1. SAR displacement model and the chirp signal in baseband

$\boldsymbol{\theta}_{\text{AIS}} = \boldsymbol{\theta}_{\text{rad}}$ is automatically satisfied when repositioning errors are lower than the radar resolution.

**Assumption 2**: The proposed model is valid for a single ship per test position. Moreover, we assume that if a ship is present at the test position then both AIS and radar signals are available. This leads to a simpler detection problem with only two hypotheses to avoid complications such as, e.g., signal conflicts with other ships (AIS collisions), false or missing AIS data, missed detections, and others.

**Assumption 3**: The bit-stuffing operation in AIS is ignored in this study, yielding to constant length AIS signals. As a consequence, the position of the information bits inside the AIS packet does not change with respect to the beginning of the message. Even if it is possible to deal with bit-stuffing, it can be neglected with a detection performance loss [1]. Our assumption facilitates our signal model and provides an upper bound of detection performance. In other words, this assumption corresponds to a best case scenario without any bit-stuffing error.

**Assumption 4**: The AIS signal model $\boldsymbol{b}(\cdot)$ depends not only on $\boldsymbol{\theta}$ but also on other parameters including Doppler, AIS bit-stuffing, time delay and ship speed. We assume here that these parameters are known by the receiver in order to obtain a simplified model $\boldsymbol{b}(\boldsymbol{\theta})$.

## III. GLRT DETECTOR FOR AIS AND RADAR DATA

In order to detect the presence of absence of a ship using AIS and radar data, we propose the following binary hypothesis testing problem

$$\begin{cases} H_0 : \alpha = \beta = 0, \text{(absence of ship)} \\ H_1 : \alpha \neq 0, \beta \neq 0, \text{(presence of ship)}. \end{cases} \quad (3)$$

Note that hypothesis $H_0$ corresponds to the absence of ship in both AIS and radar measurements whereas hypothesis $H_1$ corresponds to a situation for which the ship signature is present in both AIS and radar observations[1]. Since the two amplitudes $\alpha$ and $\beta$ are unknown, it is standard to consider the generalized likelihood ratio test (GLRT) to solve the detection problem (3). The GLRT for (3) is based on the following test statistics

$$\frac{p(\boldsymbol{y}_{\text{AIS}}, \boldsymbol{y}_{\text{rad}} | \hat{\alpha}, \hat{\beta}, \boldsymbol{\theta}, H_1)}{p(\boldsymbol{y}_{\text{AIS}}, \boldsymbol{y}_{\text{rad}} | \alpha = 0, \beta = 0, \boldsymbol{\theta}, H_0)}$$

where parameters $\hat{\alpha}$ and $\hat{\beta}$ are the maximum likelihood estimators of the signal amplitudes under hypothesis $H_1$ and $p(\boldsymbol{y}_{\text{AIS}}, \boldsymbol{y}_{\text{rad}} | \alpha, \beta, H_i)$ is the probability density function of the measurement vector $(\boldsymbol{y}_{\text{AIS}}, \boldsymbol{y}_{\text{rad}})$ at the position $\boldsymbol{\theta}$ under the hypothesis $H_i$. Assuming that the noise variances are known and that the additive noises $\boldsymbol{n}_{\text{rad}}$ and $\boldsymbol{n}_{\text{AIS}}$ are independent, the GLRT reduces to (see [15] for similar derivations)

$$T_{\text{f}} = \frac{\boldsymbol{y}_{\text{AIS}}^H \boldsymbol{P}_b(\boldsymbol{\theta}) \boldsymbol{y}_{\text{AIS}}}{\sigma_{\text{AIS}}^2} + \frac{\boldsymbol{y}_{\text{rad}}^H \boldsymbol{P}_a(\boldsymbol{\theta}) \boldsymbol{y}_{\text{rad}}}{\sigma_{\text{rad}}^2} \underset{H_0}{\overset{H_1}{\gtrless}} \eta_f \quad (4)$$

where $\boldsymbol{P}_a(\boldsymbol{\theta}) = \boldsymbol{a}(\boldsymbol{\theta}) \left[ \boldsymbol{a}(\boldsymbol{\theta})^H \boldsymbol{a}(\boldsymbol{\theta}) \right]^{-1} \boldsymbol{a}(\boldsymbol{\theta})^H$ and $\boldsymbol{P}_b(\boldsymbol{\theta}) = \boldsymbol{b}(\boldsymbol{\theta}) \left[ \boldsymbol{b}(\boldsymbol{\theta})^H \boldsymbol{b}(\boldsymbol{\theta}) \right]^{-1} \boldsymbol{b}(\boldsymbol{\theta})^H$ are the projection operators onto the subspace spanned by the vectors $\boldsymbol{a}(\boldsymbol{\theta})$ and $\boldsymbol{b}(\boldsymbol{\theta})$, and $\eta_f$ is the detection threshold. It is interesting to note that the detector (4) is a weighted sum of two independent test statistics associated with radar and AIS measurements only. This weighted sum can be viewed as the sum of the estimated signal-to-noise ratios (SNR) for the AIS and radar test statistics. Note finally that the probability of detection $P_d$ and the probability of false alarm $P_{fa}$ of the test (4) are directly related to the value of the decision threshold $\eta_f$.

When a single source of information is available, the GLRT detector (4) reduces to the matched subspace detector (MSD) [16]. For instance, in the case of radar data only, the test statistics reduces to

$$T_{\text{rad}} = \frac{\boldsymbol{y}_{\text{rad}}^H \boldsymbol{P}_a(\boldsymbol{\theta}) \boldsymbol{y}_{\text{rad}}}{\sigma_{\text{rad}}^2} \underset{H_0}{\overset{H_1}{\gtrless}} \eta_{\text{rad}} \quad (5)$$

where $\eta_{\text{rad}}$ is a detection threshold to be adjusted as a function of the desired detection performance in term of $P_d$ or $P_{fa}$.

The two detectors derived in (4) and (5) will be compared thanks to their receiver operational characteristics (ROCs), which requires the distribution of the test statistics under both hypotheses.

## IV. PERFORMANCE ANALYSIS

In the sequel, the notation $\chi_n^2(\lambda)$ indicates a chi-squared distribution with $n$ degrees of freedom and noncentrality parameter $\lambda$. We use the notation $W \sim \rho \chi_n^2(\lambda)$ for a random variable $W$ such that $W/\rho$ is distributed as a chi-squared distribution $\chi_n^2(\lambda)$. Of course, the distribution $\chi_n^2(\lambda)$ reduces to the central chi-squared distribution for $\lambda = 0$.

---

[1]The hybrid case for which the ship is present in only one of the two signatures will be considered in a future work.

## A. Distribution of the test statistic $T_f$ (radar and AIS data)

Considering known noise powers, the distributions of the joint AIS and radar detector (4) are given by

$$T_{\mathrm{f}} \sim \begin{cases} \frac{1}{2}\chi_4^2(0) & \text{under } H_0 \\ \frac{1}{2}\chi_4^2(\lambda_{\mathrm{AIS}} + \lambda_{\mathrm{rad}}) & \text{under } H_1 \end{cases} \quad (6)$$

where $\lambda_{\mathrm{AIS}} = 2\beta^2\|\boldsymbol{b}(\boldsymbol{\theta})\|^2/\sigma_{\mathrm{AIS}}^2$, $\lambda_{\mathrm{rad}} = 2\alpha^2\|\boldsymbol{a}(\boldsymbol{\theta})\|^2/\sigma_{\mathrm{rad}}^2$, and $\lambda_{\mathrm{AIS}} + \lambda_{\mathrm{rad}}$ is the noncentrality parameter of the detector distribution of the joint AIS and SAR data.

## B. Distribution of the test statistic $T_{rad}$ (radar data)

The distribution of the MSD detector in (5) (corresponding to radar only measurements) in the case of a known noise power was derived in [15].

$$T_{\mathrm{rad}} \sim \begin{cases} \frac{1}{2}\chi_2^2(0) & \text{under } H_0 \\ \frac{1}{2}\chi_2^2(\lambda_{\mathrm{rad}}) & \text{under } H_1 \end{cases} \quad (7)$$

where the noncentrality parameter $\lambda_{\mathrm{rad}}$ was defined in Section IV-A. A similar result can be obtained for the distribution of the test statistics for AIS data only.

## C. Receiver Operating Characteristics

The probability distributions derived in the previous section can be used to determine the ROCs for both detectors $T_{\mathrm{rad}}$ and $T_{\mathrm{f}}$, and thus to evaluate the potential performance gain due to the joint use of AIS and radar data. Denoting as $Q_{\chi^2}(y; n, \lambda)$ and $Q_{\chi^2}^{-1}(y; n, \lambda)$ the complementary cumulative distribution function (CCDF) and its inverse for the noncentral $\chi^2$ distribution with $n$ degrees of freedom and noncentrality parameter $\lambda$ [15], the $P_d$ and the $P_{fa}$ of both detectors can be derived as follows

AIS and radar

$$P_{fa}(T_{\mathrm{f}}) = Q_{\chi^2}(2\eta_f; 4, 0) \quad (8)$$

$$P_d(T_{\mathrm{f}}) = Q_{\chi^2}(2\eta_f; 4, \lambda_{\mathrm{AIS}} + \lambda_{\mathrm{rad}}) \quad (9)$$

Radar only

$$P_{fa}(T_{\mathrm{rad}}) = Q_{\chi^2}(2\eta_{\mathrm{rad}}; 2, 0) \quad (10)$$

$$P_d(T_{\mathrm{rad}}) = Q_{\chi^2}(2\eta_{\mathrm{rad}}; 2, \lambda_{\mathrm{rad}}). \quad (11)$$

Straightforward use of the CCDF and its inverse lead to the following equations

AIS and radar

$$P_d(T_{\mathrm{f}}) = Q_{\chi^2}(Q_{\chi^2}^{-1}(P_{fa}(T_{\mathrm{f}}); 4, 0); 4, \lambda_{\mathrm{AIS}} + \lambda_{\mathrm{rad}}) \quad (12)$$

Radar only

$$P_d(T_{\mathrm{rad}}) = Q_{\chi^2}(Q_{\chi^2}^{-1}(P_{fa}(T_{\mathrm{rad}}); 2, 0); 2, \lambda_{\mathrm{rad}}) \quad (13)$$

where (13) and (12) show that the detection performance is directly related to the noncentrality parameters $\lambda_{\mathrm{rad}}$ and $\lambda_{\mathrm{AIS}} + \lambda_{\mathrm{rad}}$. Observe that

$$2\|\alpha\boldsymbol{a}(\boldsymbol{\theta})\|^2/\sigma_{\mathrm{rad}}^2 = 2\sum_{i=1}^{N_{\mathrm{rad}}}\|\alpha a_i(\boldsymbol{\theta})\|^2/\sigma_{\mathrm{rad}}^2 = 2N_{\mathrm{rad}}\,\mathrm{SNR}_{\mathrm{rad}}$$
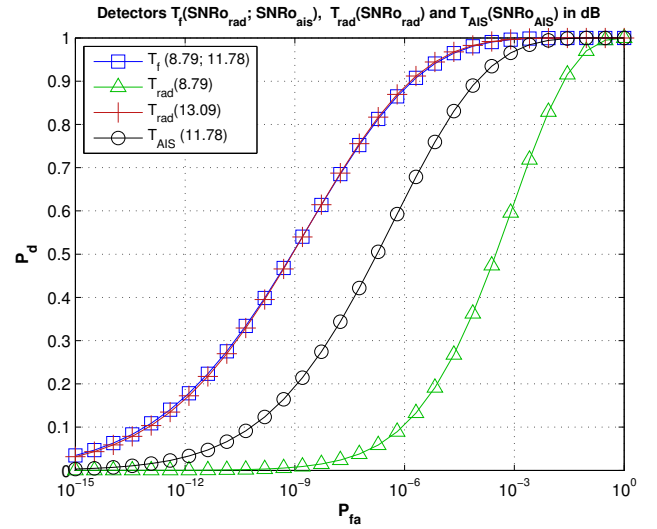


Fig. 2. ROCs of $T_{\mathrm{f}}$, $T_{\mathrm{AIS}}$ and $T_{\mathrm{rad}}$ for a small ship ($\mathrm{SNRo}_{\mathrm{rad}} = 8.79$ dB). The $T_{\mathrm{rad}}$ ROC for a bigger ship ($\mathrm{SNRo}_{\mathrm{rad}} = 13.09$ dB) is also presented for comparison.

where $N_{\mathrm{rad}}$ is the number of radar integrated samples and $\mathrm{SNR}_{\mathrm{rad}}$ the input signal-to-noise ratio of the radar samples (resp. $N_{\mathrm{AIS}}$ and $\mathrm{SNR}_{\mathrm{AIS}}$ for the AIS samples). Denoting as $\mathrm{SNRo}$ the output signal-to-noise ratio [16], we can express the noncentrality parameters as

$$\lambda_{\mathrm{rad}} = 2N_{\mathrm{rad}}\,\mathrm{SNR}_{\mathrm{rad}} = 2\,\mathrm{SNRo}_{\mathrm{rad}}$$

and

$$\lambda_{\mathrm{AIS}} = 2N_{\mathrm{AIS}}\,\mathrm{SNR}_{\mathrm{AIS}} = 2\,\mathrm{SNRo}_{\mathrm{AIS}}.$$

The different detectors are then comparable for a given target SNR expressing their performance in terms of $P_d$ as a function of $P_{fa}$ via the ROC curves.

## V. SIMULATION RESULTS

To analyze the performance of the two detectors defined before, we consider a simulation scenario (in agreement with the assumptions in II-C) with AIS and SAR signals corresponding to a single ship. The SAR system is assumed to operate with 200 pulses of $2\mu s$ and 30MHz bandwidth, yielding a total of $N_{\mathrm{rad}} = 12000$ samples. For the AIS system, the known signaling bits and the predicted message bits lend to a total of $N_{\mathrm{AIS}} = 95$. The ROCs are determined using equations (12) and (13).

The first set of experiments is presented in Fig. 2 for a small ship with a radar SNR of $-33$ dB (i.e., $\mathrm{SNRo}_{\mathrm{rad}} = 8.79$ dB) and with AIS SNR of $-8$ dB (i.e., $\mathrm{SNRo}_{\mathrm{AIS}} = 11.78$ dB). Note that we used a logarithmic scale for the X axis and a linear scale for the Y axis. The gain obtained by using both AIS and radar data (blue line with squares) can be clearly observed when compared to the detector that uses radar measurements only $T_{\mathrm{rad}}$ (green line with triangles). For reference, a detector using AIS measurements only ($T_{\mathrm{AIS}}$) is presented (black line with circles) that is also outperformed
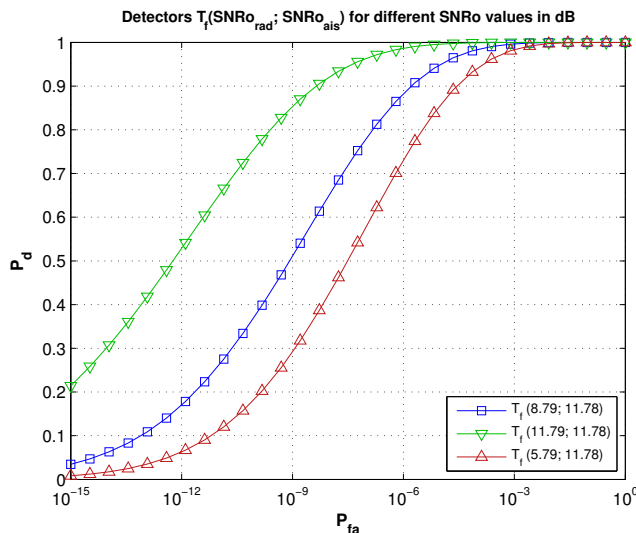
Fig. 3. ROCs of $T_{\mathrm{f}}$ for different ship sizes, i.e., different radar SNRs ($\mathrm{SNRo_{AIS}} = 11.78$ dB).

by the joint AIS/radar detector $T_{\mathrm{f}}$. Note that for a detection probability $P_d = 0.9$ the probability of false alarm of $T_{\mathrm{f}}$ is close to $P_{fa} = 10^{-6}$, whereas for $T_{\mathrm{rad}}$, we have $P_{fa}$ close to $10^{-2}$. In this example, the detector based on joint AIS/radar data provides a significative gain that allows us to detect targets $4.3$ dB smaller while keeping the same performance in terms of $P_d$ versus $P_{fa}$ (blue line with squares and red line with crosses). Note that in many studies, the performance of $T_{\mathrm{f}}$ is only compared to $T_{\mathrm{rad}}$ because the radar is more reliable than the AIS.

The second set of experiments compares ROCs associated with the joint AIS/radar detector for a fixed AIS SNR ($\mathrm{SNRo_{AIS}} = 11.78$ dB) and different radar SNRs (i.e., different ship sizes). Fig. 3 shows that the detection performance is an increasing function of the radar SNR, as expected. This kind of comparison can be made for many scenarios with tunable SNRs and processing gains for both detectors, which is the main contribution of this paper.

## VI. CONCLUSION

This paper studied a ship detector combining AIS and radar data for maritime surveillance. This problem was formulated as a binary hypothesis test that was handled using the principle of the generalized likelihood ratio detector. We derived the distribution of the resulting test statistics under both hypotheses, allowing the receiver operational characteristics to be computed in closed form. A comparison between the ROCs associated with the joint AIS/radar detector, the AIS detector and the radar detector allowed the performance gain obtained when using both sensors to be appreciated. This study was based on some important simplifying assumptions that allowed the evaluation of the detection performance of a detector that uses both AIS and radar raw data. In practice, one has to deal with the computational complexity of relocating the signals, the bit-stuffing and the different possible scenarios such as,

e.g., message collisions in AIS, multiple ships, positioning errors, missing data, and others. In a future work, our results will be validated through practical scenarios involving AIS and/or radar data. Another future work will be devoted to the fusion of radar raw signal with AIS processed data (the ship information decoded from the AIS signal), which could provide interesting results with reduced computational complexity.

## REFERENCES

[1] A. Hassanin, F. Lazaro, and S. Plass, "An advanced AIS receiver using a priori information," in *Proc. on OCEANS Conf.*, Genoa, Italy, May 2015.
[2] F. Mazzarella, M. Vespe, and C. Santamaria, "SAR ship detection and self-reporting data fusion based on traffic knowledge," *IEEE Geosci. Remote Sens. Lett.*, vol. 12, no. 8, pp. 1685–1689, Aug. 2015.
[3] "International Convention for the Safety of Life at Sea (SOLAS) Convention Chapter V," Regulation 19 - Carriage requirements for shipborne navigational systems and equipment, International Maritime Organization, 2004.
[4] *Improved satellite detection of AIS*, ITU-R Recommendation M.2169, Rev. 12/2009, 2009.
[5] M. A. Cervera, A. Ginesi, and K. Eckstein, "Satellite-based vessel automatic identification system: A feasibility and performance analysis," *Int. J. Satell. Commun. Network.*, vol. 29, pp. 117–142, 2011.
[6] J. A. Larsen and H. P. Mortensen, "In orbit validation of the AAUSAT3 SDR based AIS receiver," in *Proc. on Recent Adv. In Space Techn. RAST*, Istanbul, Turkey, Jun. 2013, pp. 487–491.
[7] T. Eriksen, A. N. Skauen, B. Narheim, O. Helleren, Ø. Olsen, and R. B. Olsen, "Tracking ship traffic with space-based AIS: Experience gained in first months of operations," in *Proc. on Int. Waterside Security Conf.*, Carrara, Italy, Nov. 2010.
[8] Maini and V. Agrawal, *Satellite Technology: Principles and Applications*. Wiley, 2010.
[9] S. Brusch, S. Lehner, T. Fritz, M. Soccorsi, A. Soloviev, and B. van Schie, "Ship surveillance with TerraSAR-X," *IEEE Trans. Geosci. Remote Sens.*, vol. 49, no. 3, pp. 1092–1103, Mar. 2011.
[10] R. Grasso, S. Mirra, A. Baldacci, J. Horstmann, M. Coffin, and M. Jarvis, "Performance assessment of a mathematical morphology ship detection algorithm for SAR images through comparison with AIS data," in *Proc. on Int. Conf. ISDA*, Pisa, Italy, Nov. 2009, pp. 602–607.
[11] S. Chaturvedi, C.-S. Yang, J.-H. Song, P. Shanmuagm, and K. Ouchi, "Preliminary technique to integrate SAR and AIS for ship detection and identification," in *Proc. on Int. Conf. APSAR*, Seoul, Korea (South), Sep. 2011.
[12] G. Margarit and A. Tabasco, "Ship classification in single-pol SAR images based on fuzzy logic," *IEEE Trans. Geosci. Remote Sens.*, vol. 49, no. 8, pp. 3129–3138, Aug. 2011.
[13] *Technical characteristics for an automatic identification system using time division multiple access in the VHF maritime mobile frequency band*, ITU-R Recommendation M.1371, Rev. 02/2014, 2014.
[14] R. Prévost, M. Coulon, D. Bonacci, J. LeMaitre, J.-P. Millerioux, and J.-Y. Tourneret, "Joint phase-recovery and demodulation-decoding of ais signals received by satellite," in *Proc. on IEEE Int. Conf. ICASSP*, Vancouver, Canada, May 2013, pp. 4913–4917.
[15] F. Vincent, O. Besson, and C. Richard, "Matched subspace detection with hypothesis dependent noise power," *IEEE Trans. Signal Process.*, vol. 56, no. 11, pp. 5713–5718, Nov. 2008.
[16] L. Scharf, *Statistical signal processing : detection, estimation, and time series analysis*. Reading, Mass: Addison-Wesley Pub. Co, 1991.